



OPEN ACCESS

EDITED BY

Mohammad Reza Khazdair,
Birjand University of Medical Sciences, Iran

REVIEWED BY

Kurtis Francis Budden,
The University of Newcastle, Australia
Stanislav Kotlyarov,
Ryazan State Medical University named after
academician I.P. Pavlov, Russia

*CORRESPONDENCE

Wenju Lu,
✉ wlu92@gzhmu.edu.cn

RECEIVED 01 August 2023

ACCEPTED 14 March 2024

PUBLISHED 09 April 2024

CITATION

Li Y, Chen J, Xing Y, Wang J, Liang Q, Zeng J,
Wang S, Yang Q, Lu J, Hu J and Lu W (2024),
Bufeï Huoxue capsule attenuates COPD-
related inflammation and regulates intestinal
microflora, metabolites.
Front. Pharmacol. 15:1270661.
doi: 10.3389/fphar.2024.1270661

COPYRIGHT

© 2024 Li, Chen, Xing, Wang, Liang, Zeng,
Wang, Yang, Lu, Hu and Lu. This is an open-
access article distributed under the terms of the
[Creative Commons Attribution License \(CC BY\)](https://creativecommons.org/licenses/by/4.0/).
The use, distribution or reproduction in other
forums is permitted, provided the original
author(s) and the copyright owner(s) are
credited and that the original publication in this
journal is cited, in accordance with accepted
academic practice. No use, distribution or
reproduction is permitted which does not
comply with these terms.

Bufeï Huoxue capsule attenuates COPD-related inflammation and regulates intestinal microflora, metabolites

Yuanyuan Li¹, Jiali Chen², Yue Xing¹, Jian Wang¹, Qiuling Liang³,
Jiamin Zeng², Siyi Wang², Qiong Yang⁴, Jianing Lu², Jieying Hu¹
and Wenju Lu^{1*}

¹Guangzhou Medicine University, Guangzhou Institute of Respiratory Health, The First Affiliated Hospital of Guangzhou Medical, Guangzhou, China, ²Guangzhou University of Chinese Medicine, Guangzhou, China, ³First Affiliated Hospital of Guangzhou Medical University, Guangzhou, China, ⁴Key Laboratory of National Health Commission for the Diagnosis and Treatment of COPD, Inner Mongolia People's Hospital, Hohhot, China

Background: Bufeï Huoxue capsule (BFHX) is widely used for the clinical treatment of chronic obstructive pulmonary disease (COPD) in China.

Objectives: The aim of this study is to explore the effects on COPD and the underlying mechanism of BFHX.

The process and methods: In this study, we established a COPD mouse model through cigarette smoke (CS) exposure in combination with lipopolysaccharide (LPS) intratracheal instillation. Subsequently, BFHX was orally administered to COPD mice, and their pulmonary function, lung pathology, and lung inflammation, including bronchoalveolar lavage fluid (BALF) cell count and classification and cytokines, were analyzed. In addition, the anti-oxidative stress ability of BFHX was detected by Western blotting, and the bacterial diversity, abundance, and fecal microbiome were examined using 16S rRNA sequencing technology.

Outcome: BFHX was shown to improve pulmonary function, suppress lung inflammation, decrease emphysema, and increase anti-oxidative stress, whereas 16S rRNA sequencing indicated that BFHX can dynamically regulate the diversity, composition, and distribution of the intestinal flora microbiome and regulate the lysine degradation and phenylalanine metabolism of COPD mice. These results highlight another treatment option for COPD and provide insights into the mechanism of BFHX.

KEYWORDS

Bufeï Huoxue capsule, chronic obstructive pulmonary disease, inflammation, intestinal flora, metabolites

Introduction

Chronic obstructive pulmonary disease (COPD) is a heterogeneous lung disease that is characterized by chronic respiratory symptoms due to abnormalities of the airways (bronchitis and bronchiolitis) and/or alveoli (emphysema), which cause persistent, progressive airflow obstruction, and it is the third most common cause of death

worldwide. As more than three-quarters of patients with COPD worldwide are from low-income and middle-income countries, it remains difficult to achieve a substantial reduction in the burden of COPD globally. Most patients with COPD suffer concomitant chronic comorbid diseases, and comorbidities directly impact on the risk of hospitalization and death (Miller et al., 2013). Treatment for COPD mainly includes abstinence from smoking, medication therapy, lung rehabilitation, oxygen therapy, and non-invasive ventilator support. Although these therapies can alleviate symptoms, reduce the frequency and severity of exacerbations, and improve health status and exercise tolerance to a certain extent, they largely fail to prevent the progression of COPD.

In recent years, mounting evidence has highlighted the role of the gut–lung axis in pathological conditions. The composition and metabolism of the microbiome influence the immune system and inflammation of the lung, whereas pulmonary disease indirectly affects the microbiome and metabolism of the gut, thus forming a vicious circle (Keely and Hansbro, 2014; Budden et al., 2017). Moreover, bowel inflammation can damage pulmonary function if left untreated, resulting in irreversible lung damage (Mateer et al., 2015; Raftery et al., 2020). Patients with COPD have a higher incidence of gastrointestinal disturbances than the general population, whereas gastrointestinal disease and ulcerative colitis are correlated with increased mortality in patients with asthma-related COPD (Ekblom et al., 2008; Mateer et al., 2015; Budden et al., 2017a; De Nuccio et al., 2022). The gut microbiome has also been shown to regulate inflammation in acute and chronic respiratory diseases, including COVID-19 and COPD (Budden et al., 2019; Bai et al., 2022).

Bufei Huoxue capsule (BFHX), which consists of *Astragalus mongholicus* Bunge, *Paeonia anomala* subsp. *veitchii* (Lynch), and *Cullen corylifolium* (L.) Medik, is widely used clinically to treat patients with COPD (Li et al., 2023). BFHX not only improves the respiratory symptoms and reduces the frequency of exacerbations in patients with COPD but also increases patients' quality of life and exercise tolerance (Chen et al., 2022). Based on these findings, we sought to establish whether BFHX functions as a treatment for COPD by regulating the gut flora. We aimed to lay a scientific foundation for further understanding the pharmacological effect of BFHX on COPD and COPD-related flora disorders.

Materials and methods

BFHX components

The BFHX capsule consists of *Astragalus exscapus* L., *Paeonia lactiflora* Pall, *Psoralea aphylla* L., *Paeonia lactiflora* Pall, and *Psoralea aphylla* L. *Astragalus exscapus* L. is dry root of *Astragalus membranaceus* (Fisch.) Bge. var. *mongholicus* (Bge.) Hsiao and *Paeonia lactiflora* Pall is dry foot of *Paeonia lactiflora* Pall. In addition, *Psoralea aphylla* L. is dry and contains mature seeds of *Psoralea corylifolia* L.

Approximately 720 g of *Astragalus exscapus* L., 540 g of *Paeonia lactiflora* Pall, and 360 g of *Psoralea aphylla* L. were boiled with 8 times the amount of water for the first time and 6 times the amount of water for the second time, for 1 h, respectively. The combined decoction was filtered and

concentrated to a relative density of 1.05–1.15 (80°C); next, ethanol was added to the decoction to achieve a 60% alcohol content for 24 h, ethyl alcohol was recycled, and the supernatant was taken to concentrate to a relative density of 1.35–1.40 (80°C). A measure of 180 g of *Paeonia Lactiflora* Pall was ground to fine powder, and then the powder was mixed well with the supernatant and ground to fine powder. The precipitation was collected and washed with 90% ethanol in turn, and then it was dried routinely to obtain the powder.

BFHX preparation and quality control were conducted as described previously (Li et al., 2023). The C-18 column (150 mm × 4.6 mm, Agilent, Italy) was equipped with a guard column for BFHX capsules and standard solutions. Three mobile phases were conducted as follows: (1) an aqueous solution containing water/acetonitrile (v/v, 68:32) (*Astragalus exscapus* L.), (2) an aqueous solution containing 0.05 mol/L potassium dihydrogen phosphate/methanol (v/v, 60:40) (*Paeonia lactiflora* Pall), and (3) an aqueous solution containing water/methanol (v/v, 52:48) (*Psoralea aphylla* L.).

Animal model and administration

Six- to eight-week-old male C57 mice were purchased from Charles River (Beijing, China) and kept under SPF conditions (12 h light/dark cycle) at a temperature of 24°C ± 2°C and 50%–60% humidity. Mice were provided water and food freely. The animal experiment was approved by the Animal Health Research Institute of Guangdong Academy of Agricultural Sciences (ethics no. SPF2020034). After a 1-week quarantine period, mice were randomly divided into the following groups: 1) control group (CTL), 2) COPD model group (MOD), 3) COPD + roflumilast (POS group, 0.5 mg/kg/d), 4) COPD + BFHX low-dose group (low group, 1.9 g/kg/d, based on the clinical dose), and 5) COPD + BFHX high-dose group (high group, 3.8 g/kg/d), n = 9 per group. All groups, except the CTL group, received cigarette smoke (CS) exposure and lipopolysaccharide (LPS) instillation, as described previously (Guan et al., 2020). Mouse airways were instilled with PBS or LPS (75 µg in 50 µL) on experimental days 1 and 14; all mice, except the CTL group, received CS exposure for 4 h with 4 h intervals. The animals were orally administered on the 61st day of the experiment for 30 days, the weights of the animals were recorded, and their states, including their hair status and movement, were observed. After administration, the animal was harvested for further analysis (n = 5–6 mice per group were analyzed).

Pulmonary function

The small animal pulmonary function instruction-forced pulmonary maneuver system (DSI, CA, United States) was used to evaluate the pulmonary function of mice. Mice were anesthetized with 1.2% avertin (0.2 mL/10 g) by intraperitoneal injection. The trachea of each mouse was cannulated and placed in the body chamber, before the pulmonary function of mice was recorded. Lung function readings were excluded from the analysis after quality control.

Bronchoalveolar lavage fluid (BALF) collection

BALF was collected by injection and aspiration of 0.8 mL of sterile saline solution repeated six times. The BALF was centrifuged at 800 rpm for 10 min at 4°C, and the supernatant was collected and stored at -80°C for cytokine assessment. The number of inflammatory cells in the BALF was counted, and the cell morphology was evaluated with hematoxylin–eosin (HE) staining. At least 200 cells on the slide were classified in a blinded manner.

Lung histology

The left lungs of the mice were inflated with paraformaldehyde fixative and excised at a 20-cm H₂O pressure. Subsequently, the lung tissues were embedded in paraffin, cut, dehydrated, and subjected to H&E staining. The mean linear intercept (MLI) of the lung tissue was measured. Periodic acid-Schiff (PAS) staining was performed to assess the level of goblet cell hyperplasia, Masson's staining was performed to evaluate collagen deposition, and α smooth muscle actin alpha (α SMA) IF staining was conducted to evaluate the expression level of the lung airway.

Enzyme-linked immunosorbent assay (ELISA)

The concentrations of monocyte chemoattractant protein-1 (MCP1) and KC (functional IL-8 in mice) in the BALF supernatant were detected using ELISA kits, according to the respective manufacturer's instructions. Briefly, the BALF supernatant was added to the ELISA plates pre-coated with capture antibodies and incubated overnight at 4°C. The ELISA plates were then washed with phosphate-buffered saline (PBS) and incubated with anti-detection antibodies at room temperature. Streptavidin-conjugated HRP was added to each well, followed by the enzyme-substrate TMB, and incubated for 10 min. The enzyme reaction was stopped by adding the 2N H₂SO₄ solution. The absorbance was read at 450 and 570 nm using a microplate reader (Gene, Hongkong, China). The concentrations of the investigated cytokines in the BALF were determined using standard curves.

Western blotting assays

Frozen lungs were lysed in lysis buffer containing the protease inhibitor PMSF (100:1). Lysates were cleared by centrifugation at 4°C for 30 min, and the total protein concentration of tissues was determined using a BCA kit (Beyotime Biotechnology, Wuhan, China). Next, 10% SDS PAGE and Western blotting were performed using a standard method, and the proteins were transferred to a polyvinylidene difluoride (PVDF) membrane (Millipore, Billerica, MA) by Western blotting (Bio-Rad Laboratories, Hercules, CA). Membranes were blocked with 5% milk and incubated with primary antibodies against β -actin, HO1, NQO1 (all from Abcam), and NOX4 (Servicebio, Wuhan, China) at 4°C overnight. The membranes were then washed in TBST followed by incubation

with goat anti-rabbit/mouse and horseradish peroxidase (HRP)-linked secondary antibodies, and the bands were detected using an enhanced chemiluminescence substrate (Tanon, Shanghai, China). The intensity of each band was determined using IPP software and was corrected to the intensity of β -actin.

Immunofluorescence

Immunofluorescence analysis was performed with the following steps: after citrate antigen was repaired, the lung sections were blocked with 10% bovine serum albumin (BSA), subjected to incubation at 4°C overnight with primary antibodies. On the second day, the slides were incubated with the fluorescent secondary antibody at 37°C for 1 h, and then the sections were restrained with 4',6'-diamino-2-phenylindole (DAPI) for nuclear location. The slides were observed under an upright fluorescence microscope (Leica, Germany).

Fecal microbiome analysis

Total fecal DNA was extracted, and 1% agarose gel electrophoresis was performed to check the extracted genomic DNA. The 16S rRNA gene V3–V4 region was amplified with the following primers (forward primer, 5'-ACTCCTACGGGAGGCAGCAG-3'; reverse primer, 5'-GGACTACHVGGGTWTCTAAT-3') by polymerase chain reaction (PCR) (ABI 3 GeneAmp® 9700, ABI, United States) before using QuantiFluor™-ST (Promega, United States) to quantify the PCR products, which were paired-end sequenced on an Illumina MiSeq instrument (Illumina, United States).

Bioinformatics and statistical analysis

Operational taxonomic units (OTUs) were divided according to different similarity levels, and bio-information from OTUs with a similarity level >97% was analyzed using the RDP classifier (V2.13) and compared with the SILVA database (V138). In the diversity analysis of samples, alpha diversity reflects the richness and diversity of the microbial community, and mothur (V1.30.2) was used to analyze the species richness and diversity of the intestinal fora. R software was employed to create curves and analyze PCA graphics. LEfSe analysis was used to analyze the correlation between OTU and gate-level annotation.

Untargeted metabolomics

Feces were collected from the rectums of mice into tubes with sterile scissors and tweezers, stored at -80°C, and then analyzed using a liquid chromatography–tandem mass spectrometry (LC–MS) system according to machine orders. Information from LC–MS was matched with metabolic public databases HMDB (<http://www.hmdb.ca/>) and KEGG (<http://www.genome.jp/kegg/compound/>) to obtain the classification of the metabolites. The annotated metabolites were then mapped to the KEGG pathway database (<http://www.kegg.jp/kegg/pathway.html>), and groups of differential metabolites were analyzed. Differential metabolite screening was performed in both groups with VIP (VIP >1) and *p*-value (*p* < 0.05).

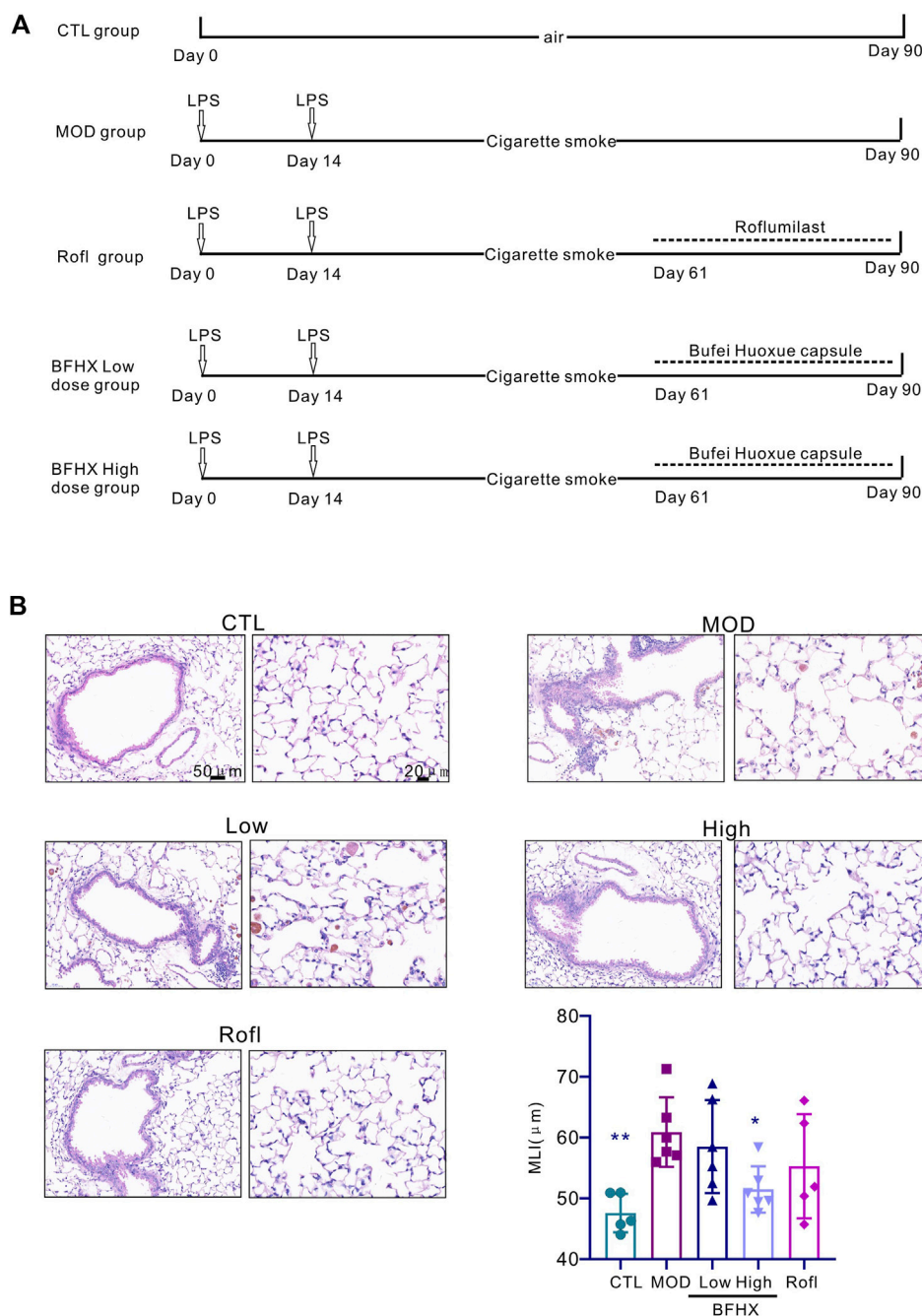


FIGURE 1 BFHX alleviates lung emphysema structural change of COPD mice. **(A)** Establishment of a COPD mouse model and treatment with BFHX. **(B)** The MLI and pathology of the mouse lung were assessed; BFHX: Bufe Huoxue capsule; results are shown as the mean ± SD, n = 4–6, vs. MOD group, **p* < 0.05, and ***p* < 0.01.

Statistical analysis

SPSS v.25.0 statistical software (IBM Corporation, USA) was used for statistical analyses. All data are represented as mean ± SEM. All assays were performed in at least three independent experiments. The statistical significance was calculated by a one-way ANOVA, which was conducted to analyze quantitative data. Dunnett’s *post hoc* test was used after one-way ANOVA analysis, for which *p* < 0.05 was considered significant.

Results

BFHX alleviates lung emphysema structural change of COPD mice

During the experiment, the status of mice was observed, and the weight of mice was recorded. CTL group mice had normal movement, stable breathing, and shiny hair, whereas CS exposure mice had decreased activity, rapid respiration, and ruffled hair. Compared

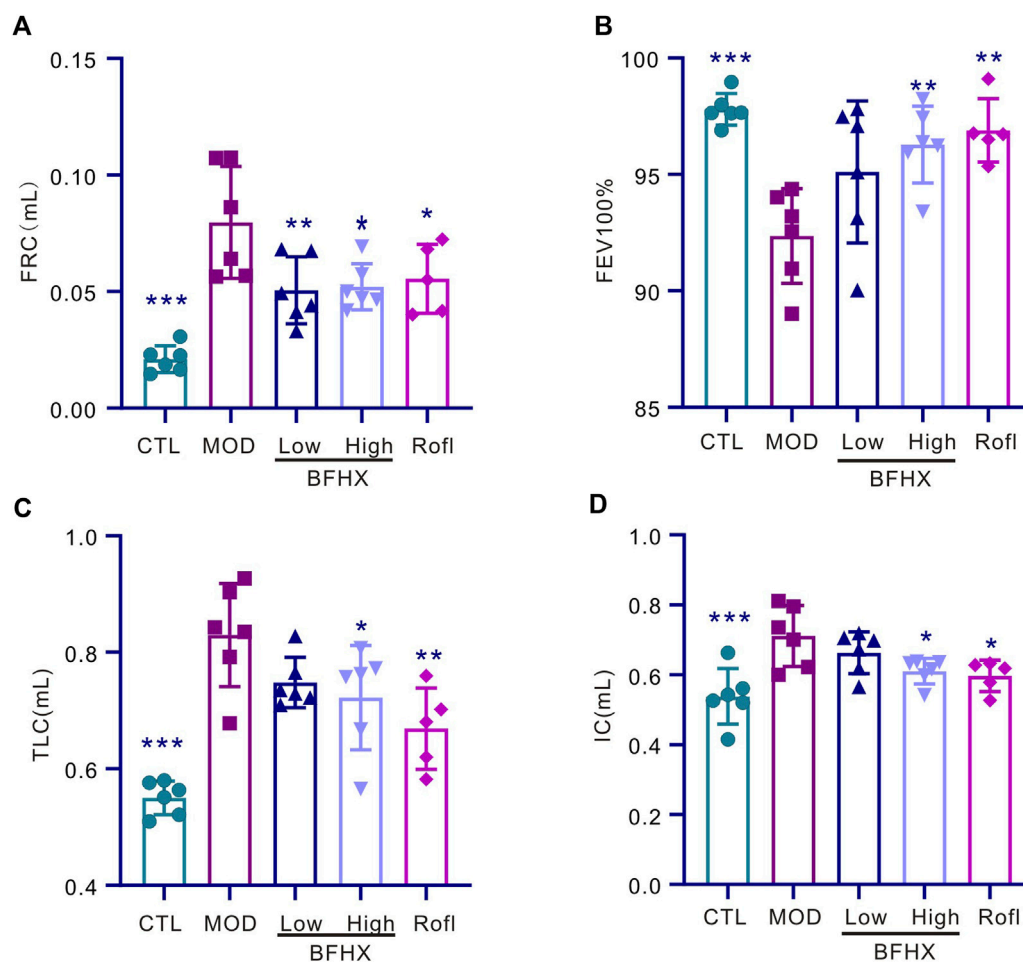


FIGURE 2
BFHX improves the pulmonary function of COPD mice. (A–D) The pulmonary function of mice, including FRC, FEV100%, TLC, and IC, was measured; FRC: functional residual capacity, FEV100%: percentage of forced vital capacity in 100 milliseconds (FEV100%), TLC: total lung capacity, IC: inspiratory capacity; results are shown as the mean \pm SD, $n = 5-6$, vs. MOD group, * $p < 0.05$, ** $p < 0.01$, and *** $p < 0.001$.

with the CTL group, CS exposure mice had slowed weight gain, and after the administration, there was no significant increase in weight gain (Supplementary Figure S1). To determine whether BFHX is harmful to other systems, the organ index (liver, spleen, and kidney) was tested. The results revealed no significant difference between the MOD and BFHX groups (Supplementary Figure S2). Airway inflammation and emphysema are the main pathological characteristics of COPD. Mice exposed to CS exposure displayed inflammation accumulation, destroyed alveoli, and increased MLI in lung tissue compared with the MOD group. The BFHX low and high groups showed reduced MLIs, indicating that BFHX reduced CS-induced emphysema (Figure 1).

BFHX improves COPD mice pulmonary function

To determine the effect of BFHX on COPD mice, we performed pulmonary function testing and pulmonary function test after administration. As shown in Figures 2A–D, CS exposure

significantly increased the functional residual capacity (FRC), percentage of forced vital capacity in 100 milliseconds (FEV100%), total lung capacity (TLC), and inspiratory capacity (IC) in the CS group. These results indicate that BFHX significantly improved the pulmonary function of COPD mice.

BFHX reduces CS-induced lung inflammation

CS induced accumulation inflammation in the cells of the lung, especially macrophages, which are the major cells in lung tissues. Acute inflammation induces acute exacerbation and promotes the progression of COPD. Consistent with the report (Arora et al., 2018), in our study, CS exposure induced inflammation accumulation in BALF (Figure 3A), predominantly macrophages (Figure 3B), whereas BFHX decreased the number of total inflammatory cells and cytokines (Figures 3E, F), indicating that BFHX suppressed CS-induced inflammation.

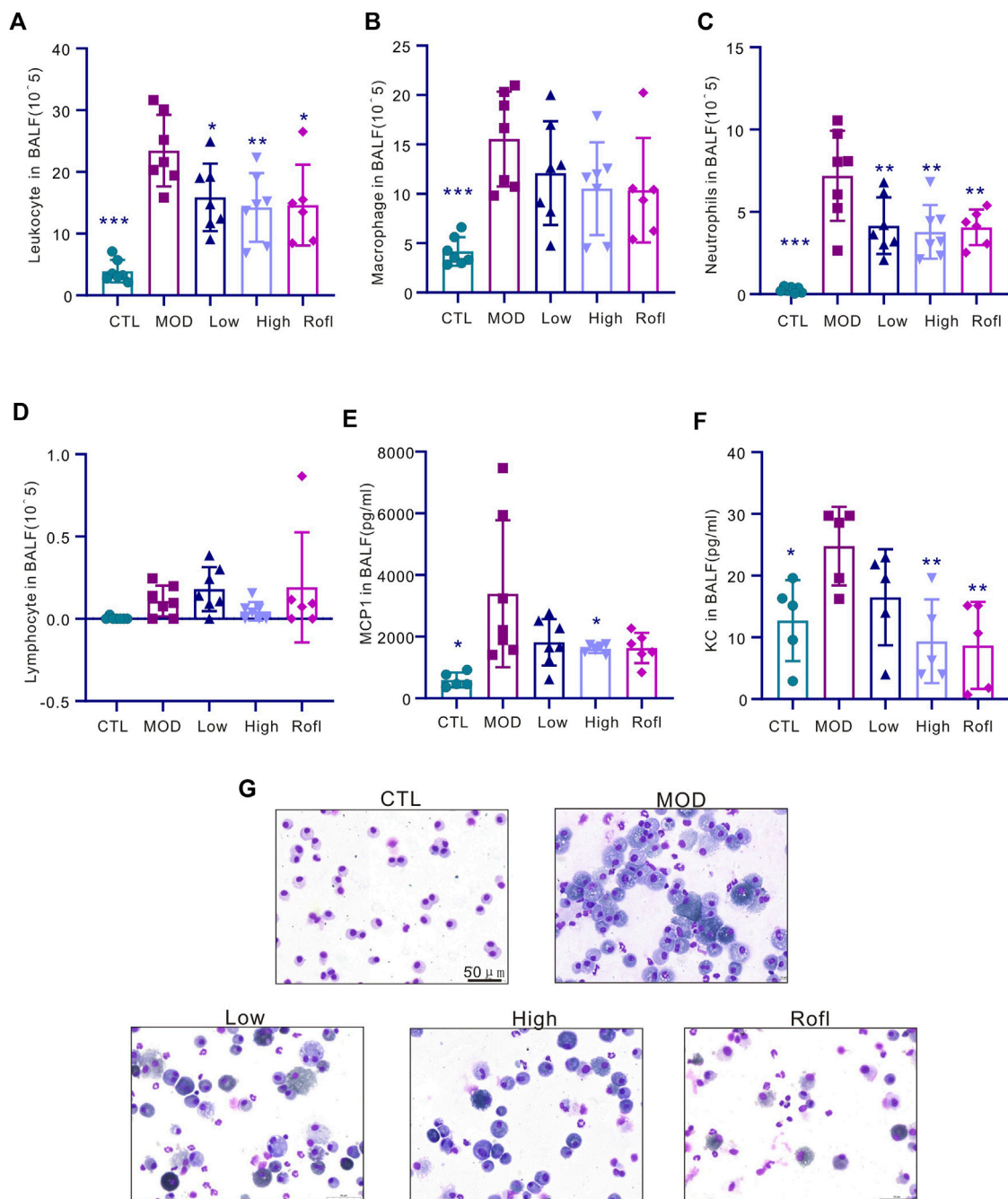


FIGURE 3 BFHX reduces CS-induced lung inflammation. (A–D) The total cell count and classification (macrophages, neutrophils, and lymphocytes) in BALF. (E) MCP1 level in BALF. (F) KC level in BALF. (G) Diagram showing cell morphologies in BALF; results are shown as the mean \pm SD, $n = 6-7$, vs. MOD group, * $p < 0.05$, ** $p < 0.01$, and *** $p < 0.001$.

BFHX inhibits CS-induced airway goblet cell hyperplasia

As mucus promotes COPD progression and airway goblet cells produce mucus with CS exposure, we next evaluated the airway goblet cell hyperplasia of COPD mice. As shown in Figure 4, PAS staining of lung tissue revealed increased and decreased goblet cells in the airways of the MOD and BFHX groups, respectively.

BFHX capsule decreases airway collagen deposition of COPD mice

Collagen deposition induces airway obstruction, which is a pathological characteristic of COPD. Therefore, we next conducted Masson's staining of lung tissue to assess collagen deposition. As shown in Figure 5, BFHX decreased collagen deposition in the airways of COPD mice. We also investigated

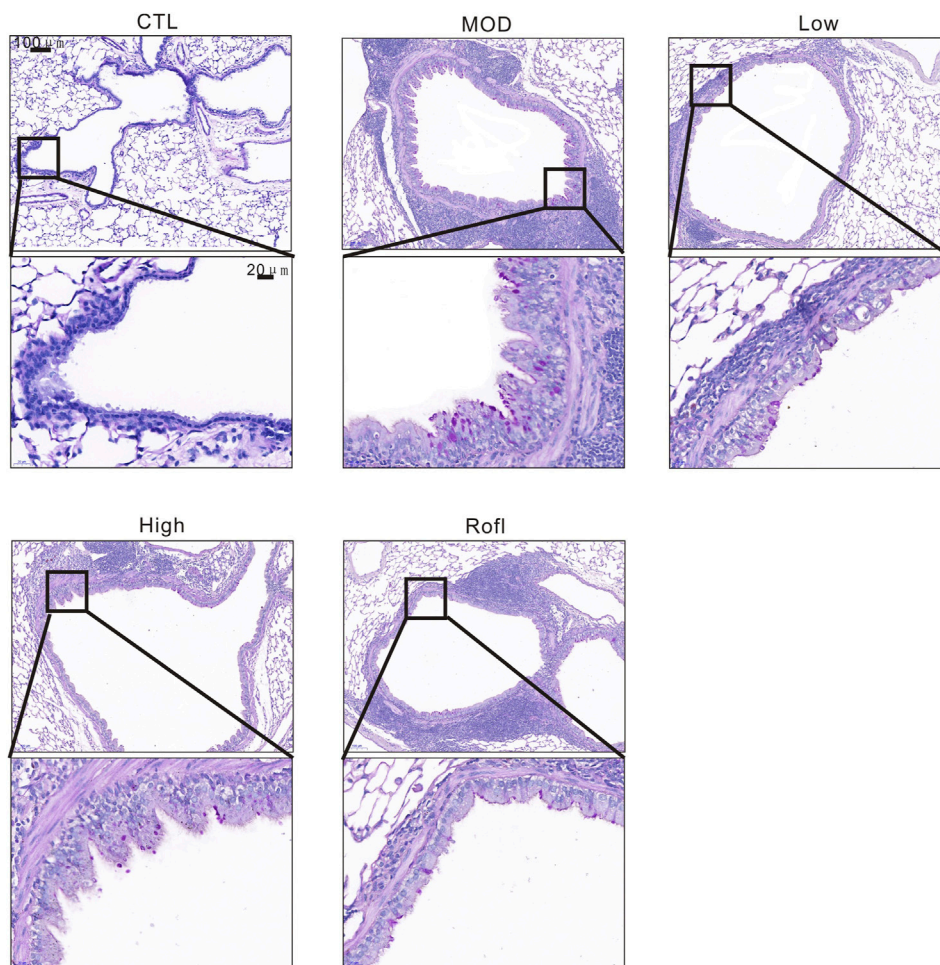


FIGURE 4
BFHX inhibits CS-induced airway goblet cell hyperplasia. PAS staining of a COPD mouse lung section.

the level of α SMA in the airways of COPD mice, as shown in [Figure 5B](#). BFHX reduced the level of α SMA induced by CS.

BFHX suppresses COPD-related oxidative stress responsive proteins *in vivo*

CS exposure can cause oxidative stress accumulation and induce chronic lung inflammation. Excessive reactive oxygen species (ROS) from CS-induced oxidative stress accelerates lung inflammation and injury in COPD, both of which produce endogenous ROS from cellular sources such as dihydronicotinamide-adenine dinucleotide phosphate (NADPH) oxidase (NOX). As shown in [Figure 6](#), BFHX decreased the level of NOX4 induced by CS exposure and LPS. In addition, the levels of antioxidant enzymes and phase 2 detoxifying enzymes, such as NADP(H): quinone oxidoreductase (NQO1) and the stress response protein heme oxygenase (HO-1), were increased in COPD mice and were found to be downregulated by BFHX.

Overall structural changes in the microbiota composition

Next, the diversity of mice was detected following the administration of BFHX. The obtained dilution curve gradually fattened, indicating a sufficient amount of sequencing data and demonstrating the rationality of the sequencing data and, indirectly, the species richness ([Supplementary Figure S3](#)). The good coverage of each group was >99.0%, indicating that the sequencing depth of the microbiome analysis meets the requirements ([Supplementary Figure S4](#)). The α diversity of the intestinal flora includes the richness and diversity of microbial communities; the Sobs index was used to evaluate the richness, and the Simpson and Shannon indices were used to evaluate the diversity of the intestinal flora of COPD mice. As shown in [Figure 7A](#), the richness of flora in the MOD group was lower, but it was increased by the BFHX administration. [Figures 7B, C](#) shows that the diversity of the bacterial population (Simpson and Shannon indices) in the MOD group was significantly lower than that in the CTL group, whereas BFHX reversed both the diversity and richness.

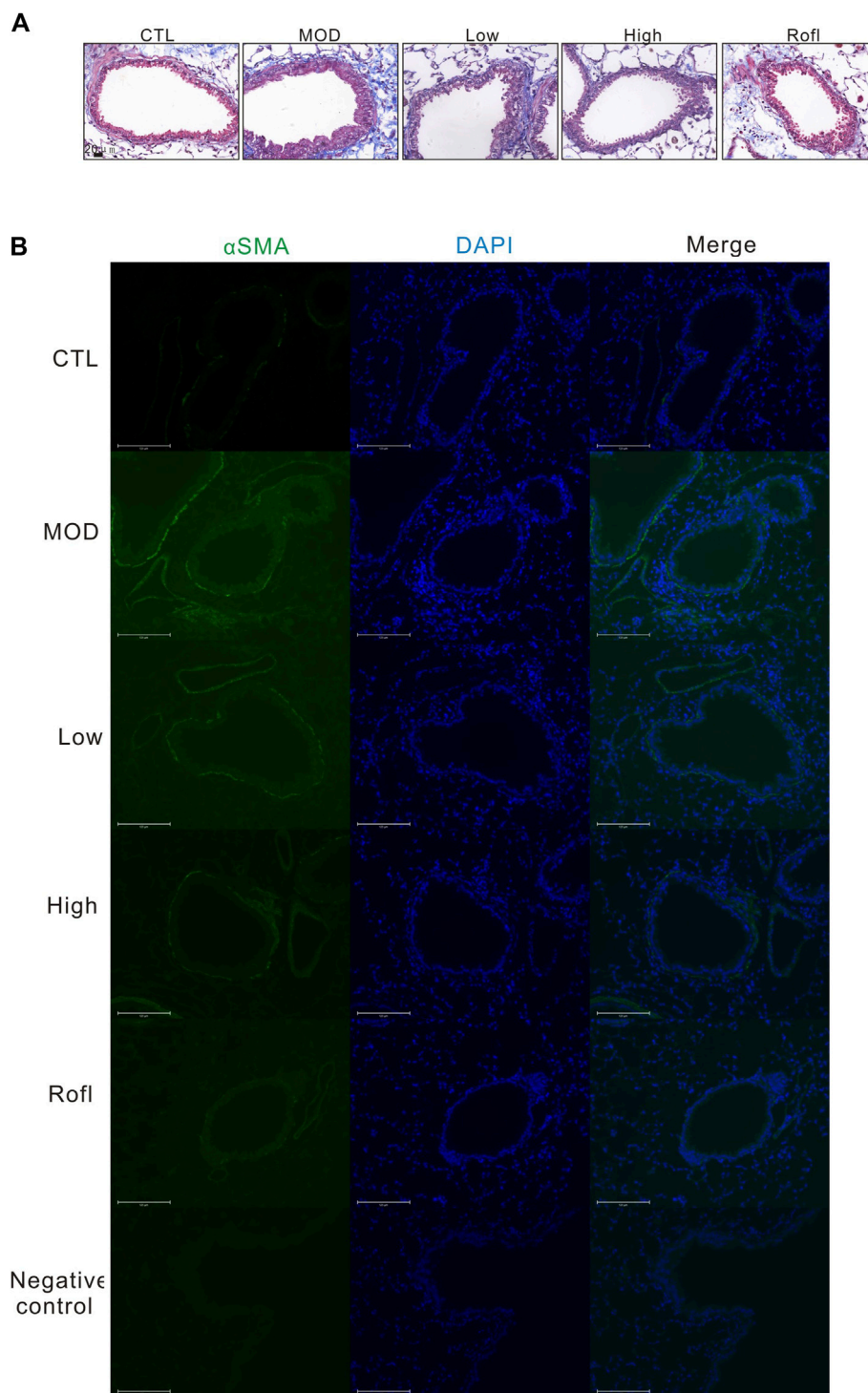


FIGURE 5 BFHX capsule decreases airway collagen deposition of COPD mice. **(A)** Masson's staining of a COPD mouse lung section. **(B)** The αSMA level of the mouse airway.

The beta diversity of each group was calculated based on cluster tree analysis, principal component analysis (PCA), and non-metric multidimensional analysis (NMDS). The PCA and hierarchical clustering tree (Figure 7D) were used to explore the

similarities and differences in intestinal flora composition in each group. The results showed that the bacterial structure of the CTL group was separated from that of the MOD group and the BFHX administration group was similar to that of the MOD

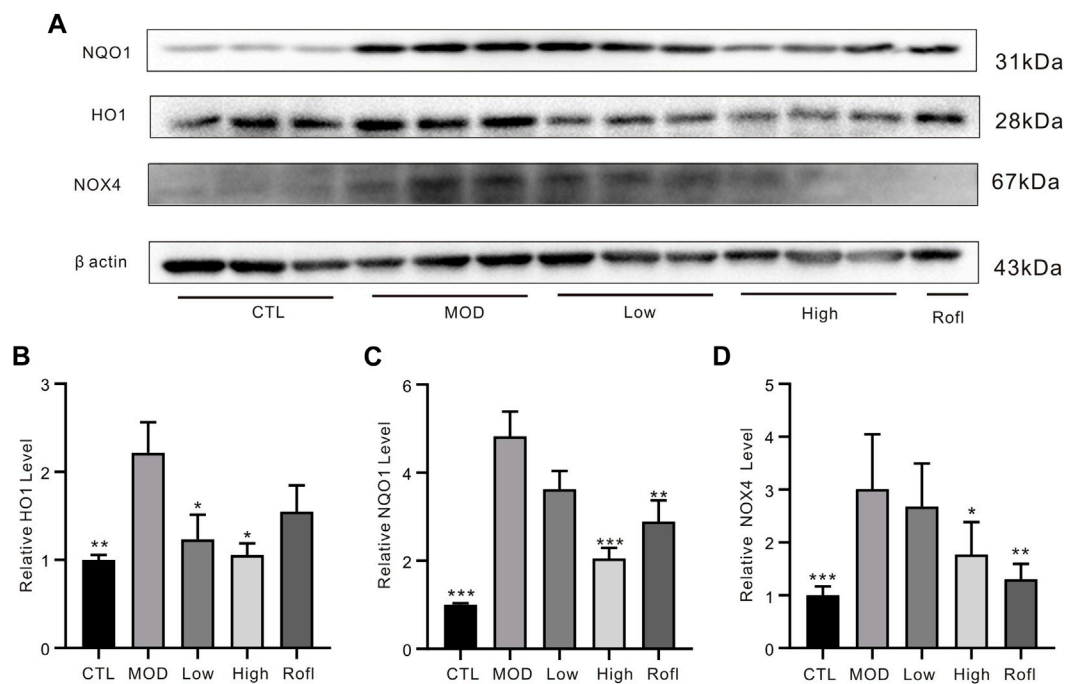


FIGURE 6 BFHX suppresses COPD-related oxidative stress responsive proteins *in vivo*. **(A)** WB bands of lung tissue. **(B)** WB band statistical results. Results are shown as the mean \pm SD, $n = 5$, vs. MOD group, * $p < 0.05$, ** $p < 0.01$, and *** $p < 0.001$.

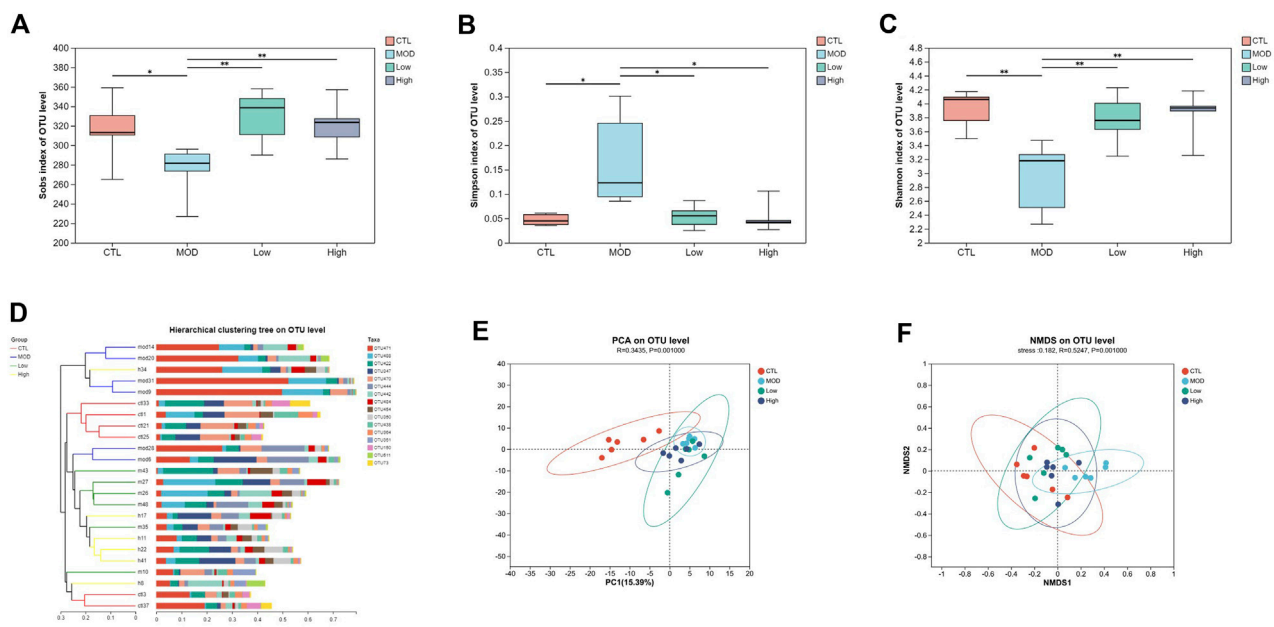


FIGURE 7 Overall structural changes in microbiota composition. **(A–C)** The Sobs, Simpson, and Shannon indices of each group. **(D)** Cluster based on the analysis of hierarchical clustering. **(E)** PCoA plots. **(F)** NMDS simplifies research objects in multidimensional space to low-dimensional space for positioning, analysis, and classification. Analyzing similarity tests (ANOSIM) were used to calculate significant differences between groups vs. MOD group, * $p < 0.05$, and ** $p < 0.01$.

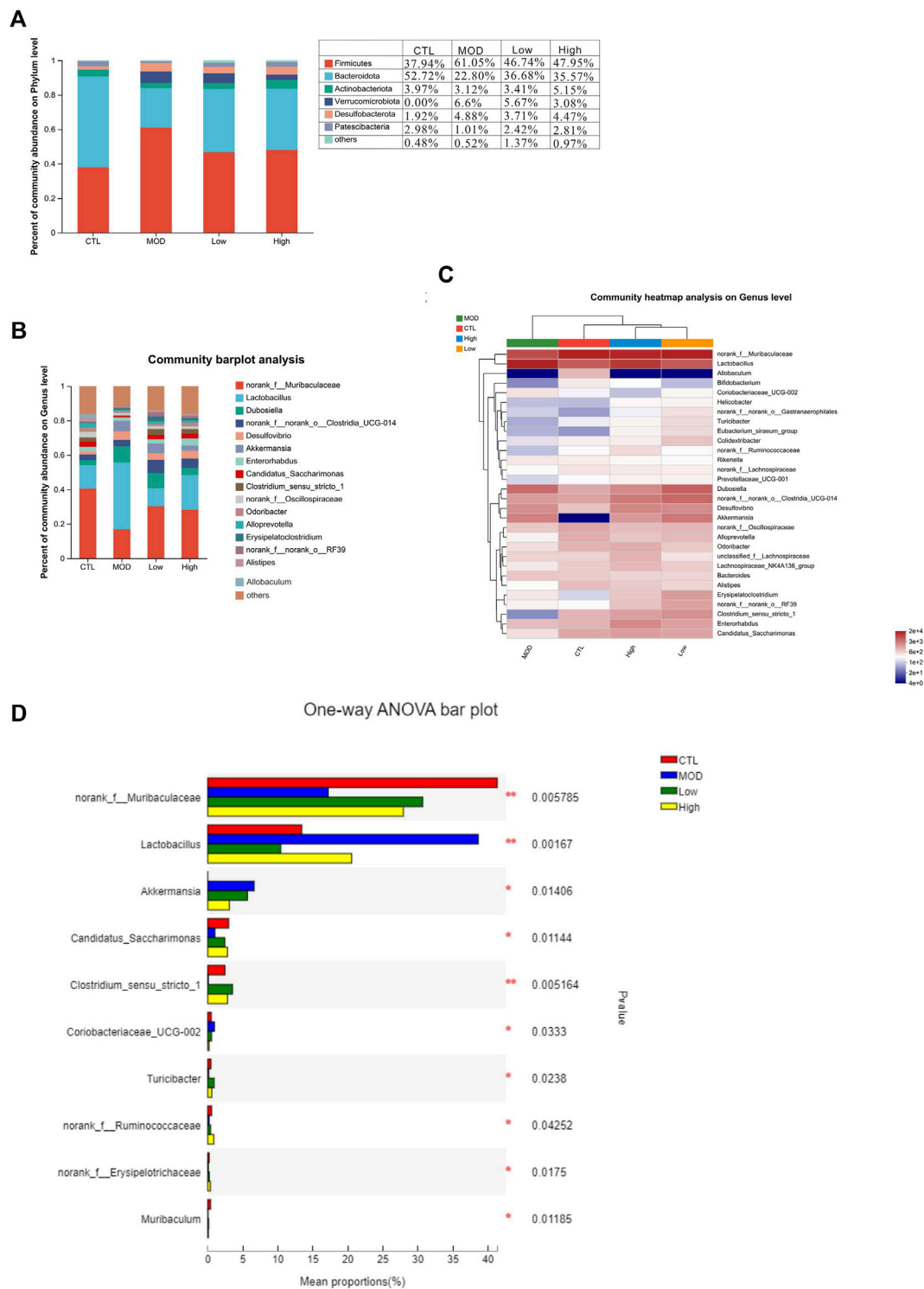
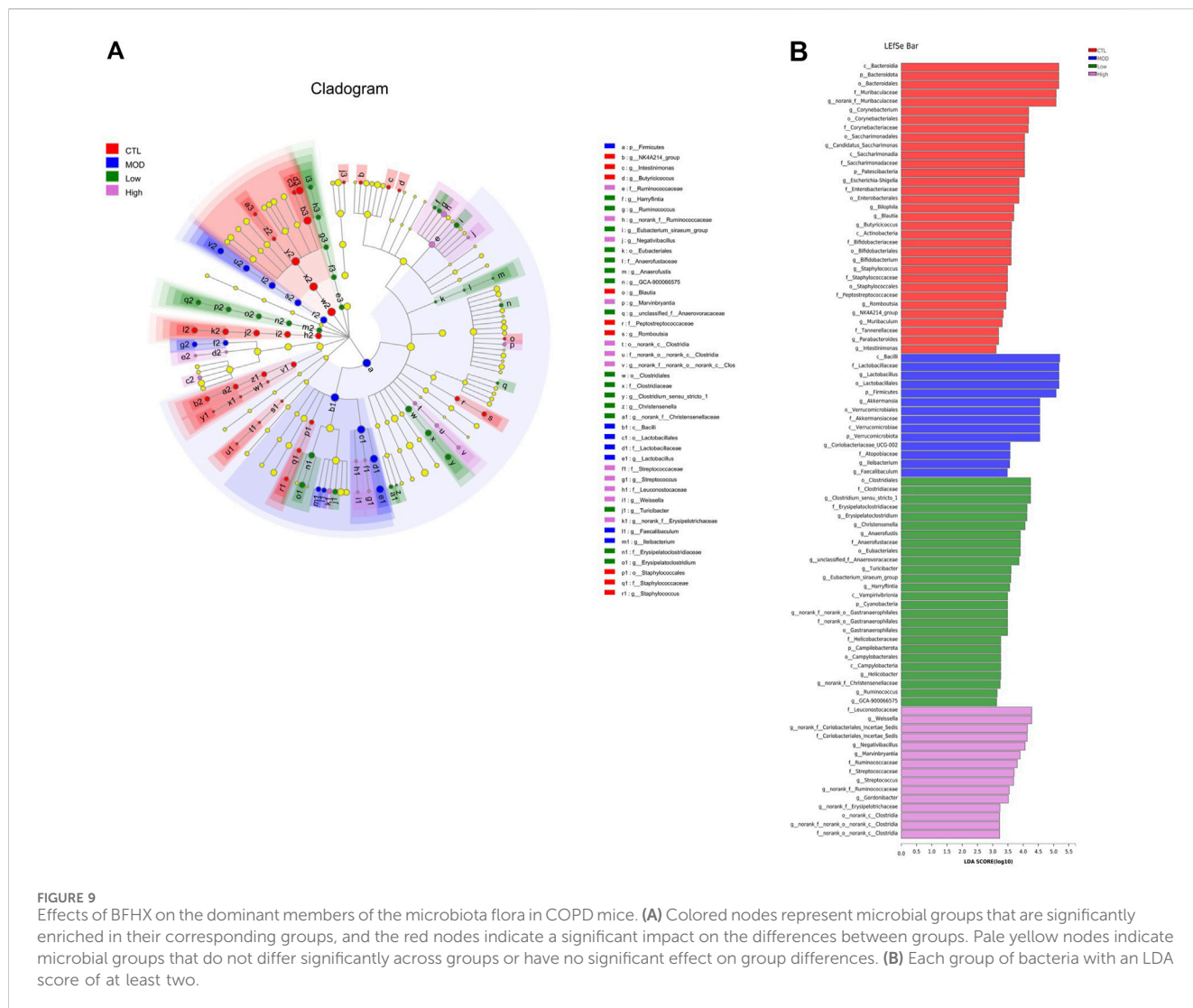


FIGURE 8 Effects of BFHX on microbial flora classification-based comparison of phylum and genus levels. * $p < 0.05$ and ** $p < 0.01$. (A,B) Intestinal flora composition analysis at the phylum and genus levels. (C) Community heatmap. (D) The mean proportions of the top ten genus differences between each group.

group. Based on the first two PCA scores, the total variations accounted for 15.39% and 9.84%, suggesting that COPD may change the percentages of bacteria in intestinal flora, and BFHX

could improve bacterial composition (Figure 7E). The NMDS of the bacterial community also showed that BFHX could improve bacterial percentage (Figure 7F).



Effect of BFHX on flora microbial classification based on the comparison of phylum and genus levels

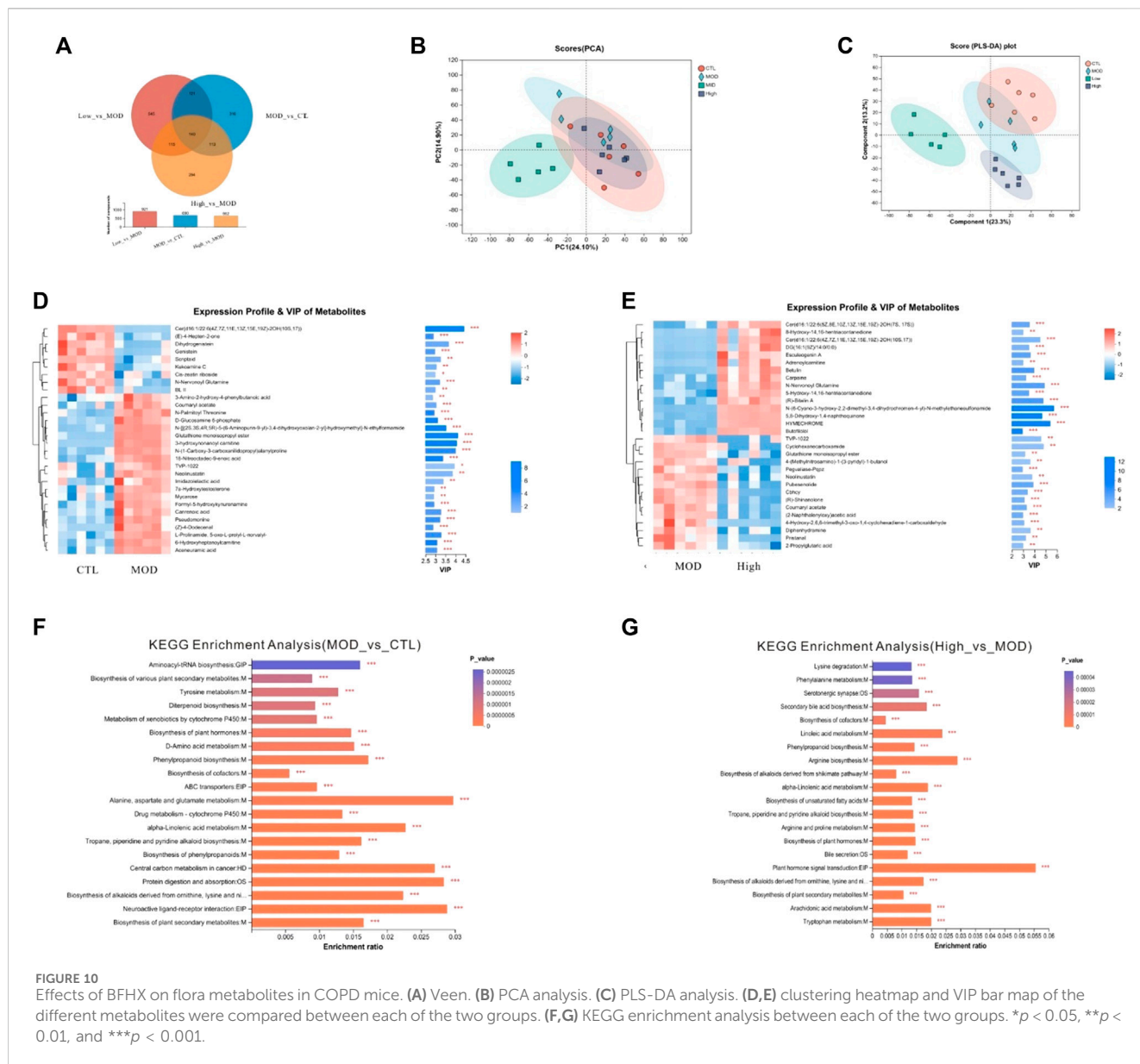
Next, a heatmap was constructed based on the top 30 dominant genera using the SILVA database. The results shown in the heatmap revealed that all 30 genera belong to six main phyla: *Firmicutes*, *Bacteroidetes*, *Actinobacteria*, *Verrucomicrobiota*, *Desulfobacterota*, and *Proteobacteria*. At the phylum level, most of the dominant genera in the CTL group belonged to *Bacteroidetes*, and most of the dominant genera in the MOD group belonged to *Firmicutes* (Figure 8A). In addition, the proportion of *Verrucomicrobiota* and *Desulfobacterota* increased while that of *Actinobacteria* decreased in the MOD group compared with the CTL group. The results revealed that BFHX reversed the proportion of bacteria at the phylum level. At the genus level, the proportions of *Murbaculaceae*, *Lactobacillus*, *Desulfuribrio*, *Clostridiumthe*, and *Akkermansia* in the CTL group decreased sharply compared to those in the MOD group, whereas the proportions of *Lactobacillus*, *Desulfuribrio*, and *Bacteroidetes* increased substantially, indicating that BFHX reversed the proportions (Figures 8B–D).

Effect of BFHX on dominant microbiota flora in COPD mice

To confirm the species differences at multiple levels, including the phylum, class, order, family, genus, and species levels, LefSe was used to identify specialized communities in flora with LDA scores ≥ 2 , as shown in Figure 9. From the phylum to the genus level, the number of dominant bacteria in each group were as follows: 33 in the CTL group, 14 in the MOD group, 26 in the low group, and 15 in the high group. In the CTL group, *Bacteroidota* dominated, whereas in the MOD, low, and high groups, *Firmicutes* dominated.

Effect of BFHX on flora metabolites in COPD mice

Next, non-targeted detection of mice fecal metabolites was performed based on LC–MS. As a result, 1784 fecal metabolites were identified in the CTL group, 1791 metabolites in the CS group, 1790 metabolites in the mid group, and 1794 metabolites in the high group. In addition, there were 17 metabolites in the CTL, mid, and high



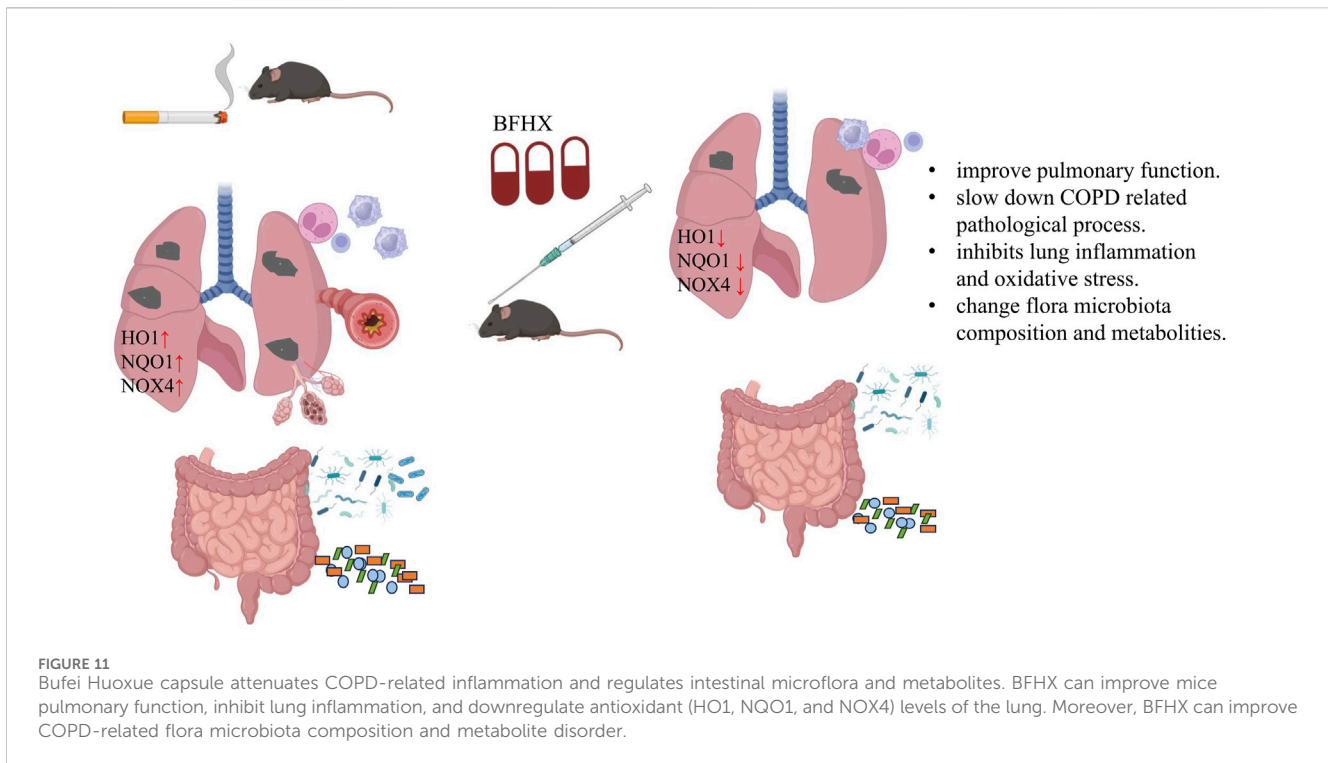
groups, and 20 metabolites in the MOD, mid, and high groups. According to different biological roles, all metabolites were classified as amino acids, vitamins and cofactors, nucleic acids, hormones and transmitters, carboxylic acids, antibiotics, steroids, organic acids, lipids, and carbohydrates. As shown in Figure 10B, PLS-DA analysis showed that the CTL, mid, and high groups' data points were clearly separated from those of the MOD group. According to the PLS-DA analysis, the fecal metabolites of mice from the high group were much closer to those of the CTL group, and lysine degradation and phenylalanine metabolism were significantly altered. The differential metabolites between each group were screened by p -value and VIP bar graph (Figures 10D-F).

Discussion

COPD, characterized by airflow limitation and airway obstruction, is a major public health burden. Indeed, the World

Health Organization predicts that COPD will become the third leading cause of mortality worldwide in 2030 (Ahmadi et al., 2015). COPD is characterized by mucus hypersecretion and inflammation, both of which promote airway obstruction. Here, we established a mouse COPD model and orally administered BFHX capsule. We found that BFHX could improve COPD mice pulmonary function, suppress COPD-related lung inflammation, inhibit CS-induced oxidative *in vitro*, relieve CS-induced intestinal flora disorder, and regulate metabolites.

The BFHX capsule consists of red peony, Psoraleae, and Astragalus. In addition to alleviating the oxidative stress and lung inflammation induced by chronic CS exposure *in vivo*, paeonol from red peony suppressed cigarette smoke extract [(CSE)-induced IL-8 *in vitro* via its antioxidant function and inhibition of the MAPKs/NF- κ B signaling (Liu et al., 2014). Astragalus containing saponins, flavonoids, and polysaccharides has been used in folk medicine for its anti-inflammatory, immune stimulation, anti-oxidative



properties (Ibrahim et al., 2013; Li et al., 2014). Psoraleae is a TCM which contains psoralea, coumarin, terpene phenolic compounds, flavonoids, etc. A growing body of research suggests that psoralea may have adequate effects in promoting bone formation and antioxidant and immune modulation activities (Wong and Rabie, 2011; Li et al., 2018) (Figure 11).

In a healthy state, there exists a delicate equilibrium between oxidants and antioxidants. However, the occurrence of hyperinflammatory injuries can disrupt this oxidative homeostasis, leading to the manifestation of various diseases (Victoni et al., 2021). Oxidative stress, resulting from an abundance of ROS or compromised endogenous antioxidant mechanisms, constitutes a primary contributing element in the development of COPD (Racanelli et al., 2018). CS induces increased oxidative stress, whereas oxidative stress causes inflammation and induces goblet cell metaplasia, producing mucus. In addition, CS is the main etiological risk factor involved in the pathogenesis of COPD. Furthermore, alongside the exogenous impacts of cigarettes, the human body generates an excessive amount of ROS during the progression of the disease (Schiffers et al., 2021; Liu et al., 2022). Consequently, oxidative stress may be a therapeutic target for patients with COPD and acute exacerbations (Barnes, 2020; Zhao and Wu, 2021). Based on the harmful effects of CS-induced oxidative stress, we checked the relative protein expression levels of HO1 and NQO1, which, compared with the CTL group, were higher following CS exposure. This excessive production of oxidative stress factors may contribute to the higher antioxidant capacity observed following exposure to harmful environments such as CS.

Under pathological conditions, there is a reciprocal influence between the gut and the lung, which occurs through the gut–lung

axis (Keely and Hansbro, 2014; Budden et al., 2017a). The reciprocal relationship between lung disease and gastrointestinal health is evident (Keely et al., 2012). In the human microbiome, 99% of the bacteria live in the gut. Under physiological conditions, the bacteria maintain intestinal homeostasis; however, under pathological conditions, the microbiome can change to facilitate a disease-promoting environment (Gomaa, 2020). Bowerman et al. (2020) identified significant differences between 28 patients diagnosed with COPD and 29 healthy individuals. *Streptococcus* sp000187445, *Streptococcus vestibularis*, and various members of the Lachnospiraceae family exhibited a significant association with diminished pulmonary function (Bowerman et al., 2020).

CS leads to gut and lung microbiota disorders, which are associated with lung inflammation and immune responses (Sze et al., 2014; Saint-Criq et al., 2020; Bai et al., 2022). In addition, the gut microbiome regulates host immune responses to respiratory infection (Trompette et al., 2018) and may contribute to the frequency of exacerbations in COPD. In circulation, the chemicals in CS directly induce inflammation and microbiome dysbiosis (Ding et al., 2021; Lai et al., 2022). Four bacterial phyla, including *Firmicutes*, *Bacteroidetes*, *Actinobacteria*, and *Proteobacteria*, dominate the healthy gut (Mathieu et al., 2018). At the phylum level, *Firmicutes* and *Bacteroidetes* are the predominant bacterial taxa in the gastrointestinal tract (Trivedi and Barve, 2020), although the relative abundance can change with disease progression and disease treatment. For example, the abundance of *Firmicutes* has been shown to increase following the administration of chemotherapy (Zhang et al., 2020). Moreover, the proportion of *Bacteroidetes* and *Firmicutes* in the gut has been shown to be

significantly different in chronic lung disease (Begley et al., 2018). Indeed, a study of 73 healthy control subjects and 99 patients with COPD showed that patients with COPD had a higher proportion of *Bacteroidetes* and a lower proportion of Firmicutes (Li et al., 2021), which is consistent with our findings. We found that the relative abundance of *Firmicutes* in the flora of COPD model mice was significantly higher than that in the normal group, whereas the relative abundance of *Bacteroidetes* was decreased. Many effective components of traditional Chinese medicine have exhibited useful biological activity and therapeutic effects on gut microflora (Yu et al., 2019; Mao et al., 2022).

Untargeted metabolites between MOD and high-dose groups were enriched in the lysine degradation and phenylalanine metabolism pathways, which is a pathway confined to the mitochondria which is ketogenic, yielding two acetyl-CoAs and reduction equivalents (Leandro and Houten, 2020). In the process of lysine degradation, cadaverine is formed. Cadaverine is the precursor of N-acetylcadaverine, and the latter has previously been associated with Crohn's disease (Diederer et al., 2020). Gut bacteria contribute to anti-inflammation in patients with multiple sclerosis via phenylalanine metabolism (Shrode et al., 2022). The deregulated tyrosine-phenylalanine axis in the urine may be a potential target for diagnostics and intervention in tuberculosis patients (Das et al., 2015). BFHX play a role in anti-inflammation and anti-oxidant effect of COPD by regulating lysine degradation and phenylalanine metabolism pathway. This study has some limitations that warrant discussion. First, we found no obvious dose-effect relationship, possibly due to improper dosage setting; the dose (1.9–3.8 g/kg/day) may be given at an ineffective interval, and the composition of BFHX that contributes to the effect is unknown. Second, although BFHX was found to improve the flora disorder, the mechanism and interaction between the effective bacteria and metabolites have not yet been explored.

In conclusion, BFHX protects mice from CS-induced lung inflammation and oxidative stress by regulating intestinal flora disorder and metabolites.

Data availability statement

The raw 16S rRNA sequencing data presented in the study are deposited in the NCBI BioProject, the accession number is PRJNA1073266.

Ethics statement

The animal study was approved by the Animal Health Research Institute of Guangdong Academy of Agricultural Sciences (ethic no. SPF2020034). The study was conducted in accordance with the local legislation and institutional requirements.

References

Ahmadi, Z., Lundström, S., Janson, C., Strang, P., Emtner, M., Currow, D. C., et al. (2015). End-of-life care in oxygen-dependent COPD and cancer: a national population-based study. *Eur. Respir. J.* 46, 1190–1193. doi:10.1183/09031936.00035915

Author contributions

YL: data curation, methodology, and writing—original draft. JC: project administration and writing—original draft. YX: data curation, formal analysis, and writing—original draft. JW: supervision and writing—review and editing. LQ: writing—original draft. JZ: writing—original draft. SW: writing—original draft and project administration. QY: writing—original draft. JL: methodology and writing—original draft. JH: writing—review and editing. WL: writing—review and editing.

Funding

The author(s) declare that financial support was received for the research, authorship, and/or publication of this article. This research was supported by the People's Hospital of Inner Mongolia Autonomous Region Open Research Fund (Grant Number R2020KF002) and National Natural Science Foundation of China (Grant Number 82241026).

Acknowledgments

The authors would like to thank the State Key Laboratory of Respiratory Disease for providing an experimental platform for the study.

Conflict of interest

The authors declare that the research was conducted in the absence of any commercial or financial relationships that could be construed as a potential conflict of interest.

Publisher's note

All claims expressed in this article are solely those of the authors and do not necessarily represent those of their affiliated organizations, or those of the publisher, the editors, and the reviewers. Any product that may be evaluated in this article, or claim that may be made by its manufacturer, is not guaranteed or endorsed by the publisher.

Supplementary material

The Supplementary Material for this article can be found online at: <https://www.frontiersin.org/articles/10.3389/fphar.2024.1270661/full#supplementary-material>

Arora, S., Dev, K., Agarwal, B., Das, P., and Syed, M. A. (2018). Macrophages: their role, activation and polarization in pulmonary diseases. *Immunobiology* 223, 383–396. doi:10.1016/j.imbio.2017.11.001

- Bai, X., Wei, H., Liu, W., Coker, O. O., Gou, H., Liu, C., et al. (2022). Cigarette smoke promotes colorectal cancer through modulation of gut microbiota and related metabolites. *Gut* 71, 2439–2450. doi:10.1136/gutjnl-2021-325021
- Barnes, P. J. (2020). Oxidative stress-based therapeutics in COPD. *Redox Biol.* 33, 101544. doi:10.1016/j.redox.2020.101544
- Begley, L., Madapoosi, S., Opron, K., Ndum, O., Baptist, A., Rysso, K., et al. (2018). Gut microbiota relationships to lung function and adult asthma phenotype: a pilot study. *BMJ Open Respir. Res.* 5, e000324. doi:10.1136/bmjresp-2018-000324
- Bowerman, K. L., Rehman, S. F., Vaughan, A., Lachner, N., Budden, K. F., Kim, R. Y., et al. (2020). Disease-associated gut microbiome and metabolome changes in patients with chronic obstructive pulmonary disease. *Nat. Commun.* 11, 5886. doi:10.1038/s41467-020-19701-0
- Budden, K. F., Gellatly, S. L., Wood, D. L., Cooper, M. A., Morrison, M., Hugenoltz, P., et al. (2017a). Emerging pathogenic links between microbiota and the gut-lung axis. *Nat. Rev. Microbiol.* 15, 55–63. doi:10.1038/nrmicro.2016.142
- Budden, K. F., Shukla, S. D., Rehman, S. F., Bowerman, K. L., Keely, S., Hugenoltz, P., et al. (2019). Functional effects of the microbiota in chronic respiratory disease. *Lancet Respir. Med.* 7, 907–920. doi:10.1016/S2213-2600(18)30510-1
- Chen, Y., Liu, C., Wang, T., Qi, J., Jia, X., Zeng, X., et al. (2022). Efficacy and safety of Bufe Huoxue capsules in the management of convalescent patients with COVID-19 infection: a multicentre, double-blind, and randomised controlled trial. *J. Ethnopharmacol.* 284, 114830. doi:10.1016/j.jep.2021.114830
- Das, M. K., Bishwal, S. C., Das, A., Dabral, D., Badireddy, V. K., Pandit, B., et al. (2015). Deregulated tyrosine-phenylalanine metabolism in pulmonary tuberculosis patients. *J. Proteome Res.* 14, 1947–1956. doi:10.1021/acs.jproteome.5b00016
- De Nuccio, F., Piscitelli, P., and Toraldo, D. M. (2022). Gut-lung microbiota interactions in chronic obstructive pulmonary disease (COPD): potential mechanisms driving progression to COPD and epidemiological data. *Lung* 200, 773–781. doi:10.1007/s00408-022-00581-8
- Dieren, K., Li, J. V., Donachie, G. E., De Meij, T. G., De Waart, D. R., Hakvoort, T. B. M., et al. (2020). Exclusive enteral nutrition mediates gut microbial and metabolic changes that are associated with remission in children with Crohn's disease. *Sci. Rep.* 10, 18879. doi:10.1038/s41598-020-75306-z
- Ding, K., Chen, J., Zhan, W., Zhang, S., Chen, Y., Long, S., et al. (2021). Microbiome links cigarette smoke-induced chronic obstructive pulmonary disease and dietary fiber via the gut-lung Axis: a narrative review. *COPD* 19, 10–17. doi:10.1080/15412555.2021.2019208
- Ekbom, A., Brandt, L., Granath, F., LöFDAHL, C. G., and Egesten, A. (2008). Increased risk of both ulcerative colitis and Crohn's disease in a population suffering from COPD. *Lung* 186, 167–172. doi:10.1007/s00408-008-9080-z
- Gomaa, E. Z. (2020). Human gut microbiota/microbiome in health and diseases: a review. *Ant. Van Leeuwenhoek* 113, 2019–2040. doi:10.1007/s10482-020-01474-7
- Guan, R., Wang, J., Cai, Z., Li, Z., Wang, L., Li, Y., et al. (2020). Hydrogen sulfide attenuates cigarette smoke-induced airway remodeling by upregulating SIRT1 signaling pathway. *Redox Biol.* 28, 101356. doi:10.1016/j.redox.2019.101356
- Ibrahim, L. F., Marzouk, M. M., Hussein, S. R., Kawashty, S. A., Mahmoud, K., and Saleh, N. A. (2013). Flavonoid constituents and biological screening of *Astragalus bombycinus* Boiss. *Nat. Prod. Res.* 27, 386–393. doi:10.1080/14786419.2012.701213
- Keely, S., and Hansbro, P. M. (2014). Lung-gut cross talk: a potential mechanism for intestinal dysfunction in patients with COPD. *Chest* 145, 199–200. doi:10.1378/chest.13-2077
- Keely, S., Talley, N. J., and Hansbro, P. M. (2012). Pulmonary-intestinal cross-talk in mucosal inflammatory disease. *Mucosal Immunol.* 5, 7–18. doi:10.1038/mi.2011.55
- Lai, H. C., Lin, T. L., Chen, T. W., Kuo, Y. L., Chang, C. J., Wu, T. R., et al. (2022). Gut microbiota modulates COPD pathogenesis: role of anti-inflammatory Parabacteroides goldsteinii lipopolysaccharide. *Gut* 71, 309–321. doi:10.1136/gutjnl-2020-322599
- Leandro, J., and Houten, S. M. (2020). The lysine degradation pathway: subcellular compartmentalization and enzyme deficiencies. *Mol. Genet. Metabolism* 131, 14–22. doi:10.1016/j.ymgme.2020.07.010
- Li, N., Dai, Z., Wang, Z., Deng, Z., Zhang, J., Pu, J., et al. (2021). Gut microbiota dysbiosis contributes to the development of chronic obstructive pulmonary disease. *Respir. Res.* 22, 274. doi:10.1186/s12931-021-01872-z
- Liu, M. H., Lin, A. H., Lee, H. F., Ko, H. K., Lee, T. S., and Kou, Y. R. (2014). Paeonol attenuates cigarette smoke-induced lung inflammation by inhibiting ROS-sensitive inflammatory signaling. *Mediat. Inflamm.* 2014, 651890. doi:10.1155/2014/651890
- Liu, X., Ma, Y., Luo, L., Zong, D., Li, H., Zeng, Z., et al. (2022). Dihydroquercetin suppresses cigarette smoke induced ferroptosis in the pathogenesis of chronic obstructive pulmonary disease by activating Nrf2-mediated pathway. *Phytomedicine* 96, 153894. doi:10.1016/j.phymed.2021.153894
- Li, X., Qu, L., Dong, Y., Han, L., Liu, E., Fang, S., et al. (2014). A review of recent research progress on the astragalus genus. *Molecules* 19, 18850–18880. doi:10.3390/molecules191118850
- Li, X., Yu, C., Hu, Y., Xia, X., Liao, Y., Zhang, J., et al. (2018). New application of psoralen and angelicin on periodontitis with anti-bacterial, anti-inflammatory, and osteogenesis effects. *Front. Cell Infect. Microbiol.* 8, 178. doi:10.3389/fcimb.2018.00178
- Li, Y., Qin, W., Liang, Q., Zeng, J., Yang, Q., Chen, Y., et al. (2023). Bufe huoxue capsule alleviates bleomycin-induced pulmonary fibrosis in mice via TGF- β 1/Smad2/3 signaling. *J. Ethnopharmacol.* 316, 116733. doi:10.1016/j.jep.2023.116733
- Mao, J., Li, Y., Bian, Q., Xuan, Y., Li, J., Wang, Z., et al. (2022). The Bufe jianpi formula improves mucosal immune function by remodeling gut microbiota through the SCFAs/GPR43/NLRP3 pathway in chronic obstructive pulmonary disease rats. *Int. J. Chron. Obstruct Pulmon. Dis.* 17, 1285–1298. doi:10.2147/COPD.S359428
- Mateer, S. W., Maltby, S., Marks, E., Foster, P. S., Horvat, J. C., Hansbro, P. M., et al. (2015). Potential mechanisms regulating pulmonary pathology in inflammatory bowel disease. *J. Leukoc. Biol.* 98, 727–737. doi:10.1189/jlb.3RU1114-563R
- Mathieu, E., Escribano-Vazquez, U., Descamps, D., Cherbuy, C., Langella, P., Riffault, S., et al. (2018). Paradigms of lung microbiota functions in health and disease, particularly, in asthma. *Front. Physiol.* 9, 1168. doi:10.3389/fphys.2018.01168
- Miller, J., Edwards, L. D., Agusti, A., Bakke, P., Calverley, P. M., Celli, B., et al. (2013). Comorbidity, systemic inflammation and outcomes in the ECLIPSE cohort. *Respir. Med.* 107, 1376–1384. doi:10.1016/j.rmed.2013.05.001
- Racaneli, A. C., Kikkers, S. A., Choi, A. M. K., and Cloonan, S. M. (2018). Autophagy and inflammation in chronic respiratory disease. *Autophagy* 14, 221–232. doi:10.1080/15548627.2017.1389823
- Raferly, A. L., Tsantikos, E., Harris, N. L., and Hibbs, M. L. (2020). Links between inflammatory bowel disease and chronic obstructive pulmonary disease. *Front. Immunol.* 11, 2144. doi:10.3389/fimmu.2020.02144
- Saint-Criq, V., Lugo-Villarino, G., and Thomas, M. (2020). Dysbiosis, malnutrition and enhanced gut-lung axis contribute to age-related respiratory diseases. *Ageing Res. Rev.* 66, 101235. doi:10.1016/j.arr.2020.101235
- Schiffers, C., Reynaert, N. L., Wouters, E. F. M., and Van Der Vliet, A. (2021). Redox dysregulation in aging and COPD: role of NOX enzymes and implications for antioxidant strategies. *Antioxidants (Basel)* 10, 1799. doi:10.3390/antiox10111799
- Shrode, R. L., Cady, N., Jensen, S. N., Borchering, N., and Mangalam, A. K. (2022). Isoflavone consumption reduces inflammation through modulation of phenylalanine and lipid metabolism. *Metabolomics* 18, 84. doi:10.1007/s11306-022-01944-1
- Sze, M. A., Meysam, A., Hogg, J. C., Sin, D. D., and Riccardo, M. (2014). A comparison between droplet digital and quantitative PCR in the analysis of bacterial 16S load in lung tissue samples from control and COPD GOLD 2. *PLOS ONE* 9, e110351. doi:10.1371/journal.pone.0110351
- Trivedi, R., and Barve, K. (2020). Gut microbiome a promising target for management of respiratory diseases. *Biochem. J.* 477, 2679–2696. doi:10.1042/BCJ20200426
- Trompette, A., Gollwitzer, E. S., Pattaroni, C., Lopez-Mejia, I. C., Riva, E., Pernot, J., et al. (2018). Dietary fiber confers protection against flu by shaping Ly6c(-) patrolling monocyte hematopoiesis and CD8(+) T cell metabolism. *Immunity* 48, 992–1005. doi:10.1016/j.immuni.2018.04.022
- Victoni, T., Barreto, E., Lagente, V., and Carvalho, V. F. (2021). Oxidative imbalance as a crucial factor in inflammatory lung diseases: could antioxidant treatment constitute a new therapeutic strategy? *Oxid. Med. Cell Longev.* 2021, 6646923. doi:10.1155/2021/6646923
- Wong, R. W., and Rabie, A. B. (2011). Effect of psoralen on bone formation. *J. Orthop. Res.* 29, 158–164. doi:10.1002/jor.21124
- Yu, L., Xing, Z. K., Mi, S. L., and Wu, X. (2019). Regulatory effect of traditional Chinese medicine on intestinal microbiota. *Zhongguo Zhong Yao Za Zhi* 44, 34–39. doi:10.19540/j.cnki.cjcm.20181101.013
- Zhang, M., Zhou, H., Xu, S., Liu, D., Cheng, Y., Gao, B., et al. (2020). The gut microbiome can be used to predict the gastrointestinal response and efficacy of lung cancer patients undergoing chemotherapy. *Ann. Palliat. Med.* 9, 4211–4227. doi:10.21037/apm-20-2183
- Zhao, X., and Wu, Y. (2021). Correlations of silent information regulator of transcription 1 (SIRT1) expression, inflammatory factors, and oxidative stress with pulmonary function in patients with acute exacerbation of chronic obstructive pulmonary disease (AECOPD). *Med. Sci. Monit.* 27, e2929046. doi:10.12659/MSM.929046